AIAA JOURNAL
Vol. 42, No. 2, February 2004

Consistent Higher-Order Dynamic Equations for Soft-Core Sandwich Beams

Vladimir S. Sokolinsky* and Steven R. Nutt†
University of Southern California, Los Angeles, California 90089-0241

The consistent higher-order dynamic equations and the corresponding continuity and boundary conditions for sandwich beams with a transversely flexible core are derived, with nonlinear acceleration fields in the core taken into account. A discretized formulation based on an efficient implicit finite difference scheme is presented and numerically validated. The higher-order analysis reveals that the dynamic magnitudes of normal stresses between the face sheets and the core increase dramatically at the boundaries of a sandwich beam, whereas the values remain at the level of response to quasi-static loading through the span, including the points of application of localized loads. The present work provides an accurate and efficient tool for the analysis of sandwich beams with a transversely flexible core subject to dynamic loads of arbitrary type, including the practical case of localized dynamic excitation.

Nomenclature

A_b	=	cross-sectional area of the lower face sheet
A_c	=	cross-sectional area of the core
A_t	=	cross-sectional area of the upper face sheet
b	=	width of sandwich beam, bottom face sheet/interface
c	=	height of the core
D	=	domain in the Euclidean space $\mathbb{R}^n$
D_h	=	set of the finite difference grid nodes in D
D_t	=	time domain, subspace in $\mathbb{R}$
$D_{\Delta t}$	=	discretized time domain
d	=	distance between the centroids of the face sheets
d_b	=	thickness of the lower face sheet
d_t	=	thickness of the upper face sheet
E_b	=	Young's modulus of the lower face sheet
E_c	=	Young's modulus of the core
E_t	=	Young's modulus of the upper face sheet
f	=	cyclic frequency, $\omega/(2\pi)$
$\boldsymbol{f}$	=	vector-function of the external loads
G_c	=	shear modulus of the core
$\boldsymbol{g}$	=	vector-function of the boundary conditions
h	=	height of sandwich beam
I_b	=	second moment of inertia of the lower face sheet
I_t	=	second moment of inertia of the upper face sheet
$\boldsymbol{K}$	=	time-independent partial differential operator in D
$\boldsymbol{K}^h$	=	$n \times n$ finite difference stiffness matrix
$\boldsymbol{k}$	=	time-independent partial differential operator on ∂D
L	=	length of sandwich beam
$\boldsymbol{M}$	=	time-independent partial differential operator in D
$M_b(x, t)$	=	localized moment load at the lower face sheet
$\boldsymbol{M}^h$	=	$n \times n$ finite difference mass matrix
$M_t(x, t)$	=	localized moment load at the upper face sheet
$\boldsymbol{m}$	=	time-independent partial differential operator on ∂D
$m_b(x, t)$	=	distributed moment load at the lower face sheet
$m_t(x, t)$	=	distributed moment load at the upper face sheet
$N_b(x, t)$	=	localized longitudinal load at the lower face sheet
N_{LF}	=	total number of localized loads applied to the sandwich beam
$N_t(x, t)$	=	localized longitudinal load at the upper face sheet
$n_b(x, t)$	=	distributed longitudinal load at the lower face sheet
$n_t(x, t)$	=	distributed longitudinal load at the upper face sheet
$P_b(x, t)$	=	localized vertical load at the lower face sheet
$P_t(x, t)$	=	localized vertical load at the upper face sheet
$p_b(x, t)$	=	distributed vertical load at the lower face sheet
$p_t(x, t)$	=	distributed vertical load at the upper face sheet
$\boldsymbol{p}(x, 0)$	=	vector-function of the initial values of main unknowns
$\boldsymbol{q}(x, 0)$	=	vector-function of the initial rate of change of the main unknowns
$\boldsymbol{r}$	=	$n \times 1$ finite difference vector comprising external loads in D_h and boundary conditions on ∂D_h
T	=	kinetic energy of sandwich beam
T_C	=	kinetic energy of the core
T_F	=	kinetic energy of the face sheets
t	=	time coordinate, top face sheet/interface
$u_c(x_c, z_c, t)$	=	longitudinal displacement of a point within the core
$u_{0b}(x_b, t)$	=	longitudinal displacement of the centroid line of the lower face sheet
$u_{0t}(x_t, t)$	=	longitudinal displacement of the centroid line of the upper face sheet
V	=	potential energy of sandwich beam
V_C	=	strain energy of the core
V_F	=	strain energy of the face sheets
$\boldsymbol{v}(x, t)$	=	5×1 vector of the main unknowns u_{0b}, u_{0t}, w_b, w_t, and τ
$\boldsymbol{v}^h$	=	$n \times 1$ finite difference vector of unknowns
$\boldsymbol{v}^{hj}$	=	finite difference vector of unknowns at the discrete time point j
$\boldsymbol{v}_k^j$	=	vector of unknowns at the kth grid node and the discrete time point j
W_{nc}	=	work of nonconservative forces
$w_b(x_b, t)$	=	vertical displacement of the centroid line of the lower face sheet
$w_{b,x}(x_b, t)$	=	rotation of the centroid line of the lower face sheet
$w_c(x_c, z_c, t)$	=	vertical displacement of a point within the core

Received 29 May 2003; revision received 5 September 2003; accepted for publication 1 October 2003.

*Research Scholar, Merwyn C. Gill Foundation Composites Center; currently Structural Scientist, Alpha Star Corporation, 5199 East Pacific Coast Highway, Suite 410, Long Beach, CA 90804. Member AIAA.

†M. C. Gill Professor, Director of Merwyn C. Gill Foundation Composites Center, Materials Science Department.

$w_t(x_t, t)$ = vertical displacement of the centroid line of the upper face sheet
$w_{t,x}(x_t, t)$ = rotation of the centroid line of the upper face sheet
x_b, y_b, z_b = local rectangular coordinates of the lower face sheet
x_c, y_c, z_c = local rectangular coordinates of the core
x_t, y_t, z_t = local rectangular coordinates of the upper face sheet
Δt = size of the discrete time interval
δ = variation of function
$\delta_D(x - x_i)$ = Dirac delta function
∂D = boundary of the domain D
∂D_h = set of the finite difference grid nodes on ∂D
ρ_b = material density of the lower face sheet
ρ_c = material density of the core
ρ_t = material density of the upper face sheet
$\sigma_{zz}(x_c, z_c, t)$ = vertical normal stress in the core
$\tau(x, t)$ = shear stress in the core
ω = circular frequency

Subscript

x = differentiation with respect to x_b, x_t, or x_c, when preceded by comma

Superscript

$\ddot{}$ = second derivative with respect to time

I. Introduction

EFFICIENT design of modern lightweight structures requires a thorough understanding of their dynamic behavior that is best modeled by systems of partial differential equations.[1]

Frostig and Baruch[2] derived partial differential equations to develop a higher-order theory describing the free vibrations of soft-core sandwich beams. The numerical structural analysis based on their model does not resort to presumed vibration modes, accounts for the interaction between the two face sheets and the soft core, and allows much closer simulation of supports used in actual practice. These distinctive features of the higher-order theory presented in Ref. 2 show important advantages over the existing sandwich models[3] for numerical simulation of the dynamic response of soft-core sandwich beams.[4]

The core of a sandwich structure is regarded as transversely flexible (soft) when the ratio of Young's moduli of the face sheets to the core is high. For structural sandwich panels, this ratio usually lies between 500 and 1000. The characteristic property of sandwich beams with a transversely flexible core is the vertical flexibility that causes nonlinear longitudinal and vertical displacement patterns in the core.[2] The model of Frostig and Baruch[2] is based on the displacement fields, which vary nonlinearly with the height of the core, both in the longitudinal and vertical directions. At the same time, the acceleration fields of the core in the longitudinal and vertical directions are assumed to vary linearly with height. In this respect, the higher-order dynamic model in Ref. 2 is inherently inconsistent.

This inconsistency has only a minor effect on the accuracy of the numerical results when simulating free vibrations of sandwich beams because the inertia loads exerted on a freely vibrating sandwich beam are predominantly uniformly distributed along the structure (except in the vicinity of structural supports). The localized nonlinearities arising in the vicinity of supporting points are small and can be disregarded without loss of accuracy.

However, when some important practical cases are considered, such as the free vibrations of delaminated sandwich beams[5] or forced response of sandwich beams subject to localized loads, limitations of the model presented in Ref. 2 become apparent. In such circumstances, accounting for the nonlinear acceleration fields in the transversely flexible core becomes essential for the analysis because the inertia loads exerted on the sandwich beams are nonuniformly distributed along the span.

The aim of the present paper is to develop a consistent higher-order formulation that can be used for the analysis of soft-core sandwich beams subject to external dynamic excitations of any type, including localized loads, and for the free vibration analysis of delaminated sandwich beams.

In what follows, a consistent higher-order dynamic formulation for soft-core sandwich beams is developed in terms of the system of governing partial differential equations and the corresponding continuity and boundary conditions. Next, the discretization of the derived continuous formulation based on the efficient implicit finite difference scheme is outlined, followed by a qualitative and quantitative validation of the developed formulation. Finally, numerical examples of the forced response of cantilevered and simply supported soft-core sandwich beams subject to localized harmonic loads are presented to illustrate numerical applications of the developed formulation.

II. Mathematical Formulation

A. Assumptions

The assumptions of the consistent higher-order formulation under discussion follow in general the concept set forth in Refs. 6–8 (Fig. 1). According to this concept, the thin face sheets of a sandwich beam are modeled as ordinary beams with negligible shear strains that follow Euler–Bernoulli assumptions and are subjected to small deformations. The transversely flexible core layer is considered as an antiplane two-dimensional isotropic elastic medium with small deformations where its height may change under loading and its cross section does not remain planar (nonlinear displacement fields in the core). Here an antiplane core implies that the Young's modulus in planes parallel to the face sheets is zero, but the shear and Young's moduli in planes perpendicular to the face sheets are finite.[9] The interface layers between the face sheets and the core are assumed to be infinitely rigid, which provides perfect continuity of the deformations at the interfaces.

In the consistent formulation under consideration, the static deformation fields of the face sheets and the core are generalized to include time variation, which is a standard practice in structural mechanics.[10] Thus, the acceleration fields of the upper and lower face sheets vary linearly with height, whereas the core acceleration fields vary nonlinearly with height in both the longitudinal and vertical directions.

Note that because the face sheets and the core of a sandwich structure are modeled using such fundamental mechanical

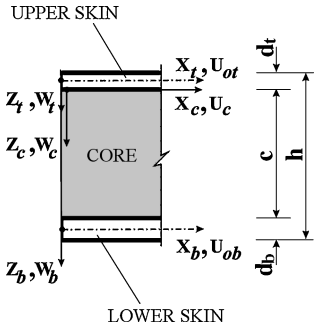

a) Geometry

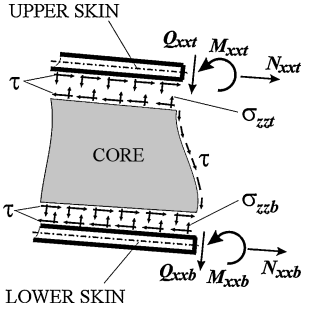

b) Internal stresses and stress resultants

Fig. 1 Sandwich beam conventions.

approximations as the beam model and the two-dimensional isotropic elastic medium, respectively, all of the usual types of viscous or structural damping can be readily incorporated in future analysis.

B. Equations of Motion

The governing differential equations and the corresponding continuity and boundary conditions are derived here via application of the extended Hamilton variational principle (see Ref. 11):

$$\int_{t_1}^{t_2} (\delta T - \delta V + \delta W_{nc})\,\mathrm{d}t = 0, \qquad \delta \boldsymbol{v}(t_1) = \delta \boldsymbol{v}(t_2) = 0 \tag{1}$$

The strain and kinetic energy of the isotropic face sheets, respectively, read

$$V_F = \frac{1}{2}\int_0^L \left(EA_t u_{0t,x}^2 + EI_t w_{t,xx}^2 + EA_b u_{0b,x}^2 + EI_b w_{b,xx}^2\right)\mathrm{d}x \tag{2}$$

$$T_F = \frac{1}{2}\int_0^L \left\{\left[\rho_t A_t\left(\dot{u}_{0t}^2 + \dot{w}_t^2\right) + \rho_t I_t \dot{w}_{t,x}^2\right] + \left[\rho_b A_b\left(\dot{u}_{0b}^2 + \dot{w}_b^2\right) + \rho_b I_b \dot{w}_{b,x}^2\right]\right\}\mathrm{d}x \tag{3}$$

Reissner[6] has shown that if the core is assumed to be antiplane,[9] the two partial differential equations describing equilibrium can be uncoupled and solved analytically for the longitudinal and vertical displacements (also see Refs. 7 and 8). The resultant expressions, which are generalized here to include the time parameter, are

$$u_c(x_c, z_c, t) = \frac{z_c}{G_c}\tau - \frac{z_c^2(3c - 2z_c)}{12E_c}\tau_{,xx} - \frac{z_c^2}{2c}w_{b,x} + \left(\frac{z_c^2}{2c} - z_c - \frac{d_t}{2}\right)w_{t,x} + u_{0t} \tag{4}$$

$$w_c(x_c, z_c, t) = -\frac{z_c(z_c - c)}{2E_c}\tau_{,x} + \frac{z_c}{c}(w_b - w_t) + w_t \tag{5}$$

Therefore, the strain and kinetic energy of the isotropic transversely flexible core are

$$V_C = \frac{1}{2}\int_0^L b\left[\frac{c}{G_c}\tau^2 + \frac{c^3}{12E_c}\tau_{,x}^2 + \frac{E_c}{c}\left(w_t^2 + w_b^2 - 2w_t w_b\right)\right]\mathrm{d}x \tag{6}$$

$$\begin{aligned} T_C = \frac{1}{2}\int_0^L b\rho_c \Bigg\{ & \left(\frac{c^3}{3G_c^2}\right)\dot{\tau}^2 + \left(\frac{13c^7}{5040}E_c^2\right)\dot{\tau}_{,xx}^2 + \left(\frac{c^3}{20}\right)\dot{w}_{b,x}^2 \\ & + \left[\left(\frac{2}{15}\right)c^3 + \left(\frac{d_t}{3}\right)c^2 + \left(\frac{d_t^2}{4}\right)c\right]\dot{w}_{t,x}^2 + c\dot{u}_{0t}^2 \\ & - \left(\frac{7c^5}{120E_cG_c}\right)\dot{\tau}\dot{\tau}_{,xx} - \left(\frac{c^3}{4G_c}\right)\dot{\tau}\dot{w}_{b,x} \\ & - \left[2\left(\frac{5c^3}{24} + \frac{c^2d_t}{4}\right)\Big/ G_c\right]\dot{\tau}\dot{w}_{t,x} + \left(\frac{c^2}{G_c}\right)\dot{\tau}\dot{u}_{0t} \\ & + \left(\frac{c^5}{45E_c}\right)\dot{\tau}_{,xx}\dot{w}_{b,x} + \left[\left(\frac{13c^5}{360} + \frac{c^4d_t}{24}\right)\Big/ E_c\right]\dot{\tau}_{,xx}\dot{w}_{t,x} \\ & - \left(\frac{c^4}{12E_c}\right)\dot{\tau}_{,xx}\dot{u}_{0t} + \left(\frac{3c^3}{20} + \frac{c^2d_t}{6}\right)\dot{w}_{b,x}\dot{w}_{t,x} - \left(\frac{c^2}{3}\right)\dot{w}_{b,x}\dot{u}_{0t} \\ & - \left(\frac{2c^2}{3} + d_t c\right)\dot{w}_{t,x}\dot{u}_{0t} + \left(\frac{c^5}{120E_c^2}\right)\dot{\tau}_{,x}^2 + \left(\frac{c}{3}\right)\dot{w}_t^2 + \left(\frac{c}{3}\right)\dot{w}_b^2 \\ & + \left(\frac{c^3}{12E_c}\right)\dot{\tau}_{,x}\dot{w}_t + \left(\frac{c^3}{12E_c}\right)\dot{\tau}_{,x}\dot{w}_b + \left(\frac{c}{3}\right)\dot{w}_t\dot{w}_b\Bigg\}\mathrm{d}x \end{aligned} \tag{7}$$

The work due to the nonconservative external forces acting on a sandwich beam is

$$\begin{aligned} W_{nc} = \int_0^L \Bigg\{ & n_t(x,t)u_{0t} + n_b(x,t)u_{0b} + p_t(x,t)w_t + p_b(x,t)w_b \\ & + m_t(x,t)\frac{\partial w_t}{\partial x} + m_b(x,t)\frac{\partial w_b}{\partial x} + \sum_{i=1}^{i=N_{LF}}[N_{ti}(x,t)u_{0t} \\ & + N_{bi}(x,t)u_{0b} + P_{ti}(x,t)w_t + P_{bi}(x,t)w_b + M_{ti}(x,t)w_{t,x} \\ & + M_{bi}(x,t)w_{b,x}]\delta_D(x - x_i)\Bigg\}\mathrm{d}x \end{aligned} \tag{8}$$

The use of the extended Hamilton principle in Eq. (1) is justified only if there is kinematic compatibility in the longitudinal and vertical directions between the face sheets and core at the top and bottom interface layers of a sandwich beam. As shown by Benson and Mayers,[7] Eqs. (4) and (5) assure the vertical compatibility at both interfaces and the longitudinal compatibility only at the upper interface layer. Thus, to ensure compatibility between the lower face sheet and the core in the longitudinal direction, the following condition must be added to the functional in Eq. (1):

$$u_c(x_c, z_c = c, t) = u_{0b}(x_b, t) + (d_b/2)w_{b,x}(x_b, t) \tag{9}$$

which, after the use of Eq. (4) and multiplication by b, yields the following auxiliary condition:

$$bu_{0b} - bu_{0t} - (bc/G_c)\tau + \left(bc^3\big/12E_c\right)\tau_{,xx} + [b(c + d_t)/2]w_{t,x} + [b(c + d_b)/2]w_{b,x} = 0 \tag{10}$$

The constrained variation of the Eq. (1) is accomplished using the Lagrangian multiplier method.[12,13] This procedure produces the system of governing partial differential equations along with the continuity and boundary conditions in terms of the longitudinal, u_{0t} and u_{0b}, and vertical, w_t and w_b, displacements of the face sheets, shear stress in the core, τ, and the Lagrange multiplier. The Lagrange multiplier can be shown to be the shear stress τ in the core (compare with Ref. 7) that permits representation of the higher-order formulation in terms of the vector $\boldsymbol{v}(x,t) = \{u_{0b}, u_{0t}, w_b, w_t, \tau\}$.

Thus, the higher-order dynamic equations for sandwich beams with a soft isotropic core and isotropic face sheets, which take into consideration the nonlinear acceleration fields in the core, are

$$\begin{aligned} & EA_t u_{0t,xx} + b\tau - \rho_t A_t \ddot{u}_{0t} - \rho_c A_c[(13/35)\ddot{u}_{0t} + (9/70)\ddot{u}_{0b} \\ & \quad - (1/210)(11c + 39d_t)\ddot{w}_{t,x} + (1/420)(13c + 27d_b)\ddot{w}_{b,x} \\ & \quad + (3/140)(c/G_c)\ddot{\tau}] = -n_t \end{aligned} \tag{11}$$

$$\begin{aligned} & EA_b u_{0b,xx} - b\tau - \rho_b A_b \ddot{u}_{0b} - \rho_c A_c[(9/70)\ddot{u}_{0t} + (13/35)\ddot{u}_{0b} \\ & \quad - (1/420)(13c + 27d_t)\ddot{w}_{t,x} + (1/210)(11c + 39d_b)\ddot{w}_{b,x} \\ & \quad - (3/140)(c/G_c)\ddot{\tau}] = -n_b \end{aligned} \tag{12}$$

$$\begin{aligned} & EI_t w_{t,xxxx} + (bE_c/c)(w_t - w_b) - (1/2)b(c + d_t)\tau_{,x} + \rho_t A_t \ddot{w}_t \\ & \quad - \rho_t I_t \ddot{w}_{t,xx} + \rho_c A_c\Big\{(1/210)(11c + 39d_t)\ddot{u}_{0t,x} \\ & \quad + (1/420)(13c + 27d_t)\ddot{u}_{0b,x} + (1/3)\ddot{w}_t \\ & \quad - (1/420)\left(4c^2 + 22cd_t + 39d_t^2\right)\ddot{w}_{t,xx} + (1/6)\ddot{w}_b \\ & \quad + (1/840)\left[6c^2 + 13c(d_t + d_b) + 27d_t d_b\right]\ddot{w}_{b,xx} \\ & \quad + (1/840)(c/E_cG_c)[35cG_c + E_c(2c + 9d_t)]\ddot{\tau}_{,x}\Big\} = p_t - m_{t,x} \end{aligned} \tag{13}$$

$$
\begin{aligned}
&EI_b w_{b,xxxx} - (bE_c/c)(w_t - w_b) - (1/2)b(c+d_b)\tau_{,x} + \rho_b A_b \ddot{w}_b \\
&\quad - \rho_b I_b \ddot{w}_{b,xx} - \rho_c A_c \Big\{ (1/420)(13c + 27d_b)\ddot{u}_{0t,x} \\
&\quad + (1/210)(11c + 39d_b)\ddot{u}_{0b,x} - (1/6)\ddot{w}_t \\
&\quad - (1/840)\Big[6c^2 + 13c(d_t + d_b) + 27d_t d_b\Big]\ddot{w}_{t,xx} - (1/3)\ddot{w}_b \\
&\quad + (1/420)\Big[4c^2 + 22cd_b + 39d_b^2\Big]\ddot{w}_{b,xx} \\
&\quad - (1/840)(c/E_c G_c)[35cG_c + E_c(2c + 9d_b)]\ddot{\tau}_{,x} \Big\} = p_b - m_{b,x}
\end{aligned} \tag{14}
$$

$$
\begin{aligned}
&bu_{0t} - bu_{0b} - [b(c+d_t)/2]w_{t,x} - [b(c+d_b)/2]w_{b,x} \\
&\quad - \Big(bc^3 \Big/ 12E_c\Big)\tau_{,xx} + (bc/G_c)\tau + (A_c\rho_c c/E_c G_c) \\
&\quad \times \{(1/140)(14G_c - 3E_c)(\ddot{u}_{0t} - \ddot{u}_{0b}) - (1/840) \\
&\quad \times [G_c(7c + 42d_t) - E_c(2c + 9d_t)]\ddot{w}_{t,x} \\
&\quad - (1/840)[G_c(7c + 42d_b) - E_c(2c + 9d_b)]\ddot{w}_{b,x} \\
&\quad + (1/210)(c/G_c)[21G_c - E_c]\ddot{\tau}\} = 0
\end{aligned} \tag{15}
$$

The first four equations just derived represent dynamic equilibrium in the horizontal [Eqs. (11) and (12)] and vertical [Eqs. (13) and (14)] directions of the face sheets supported by a soft core. The fifth equation [Eq. (15)] is a combination of the compatibility condition in the longitudinal direction at the lower interface layer, which can be verified by comparison between Eq. (10) and the first six terms in Eq. (15), and the following identity resulting from the variational procedure:

$$
\begin{aligned}
&(A_c\rho_c/E_c G_c)\Big\{(1/140)c(14G_c - 3E_c)(\ddot{u}_{0t} - \ddot{u}_{0b}) \\
&\quad - (1/840)c[G_c(7c + 42d_t) - E_c(2c + 9d_t)]\ddot{w}_{t,x} \\
&\quad - (1/840)c[G_c(7c + 42d_b) - E_c(2c + 9d_b)]\ddot{w}_{b,x} \\
&\quad + (1/210)\Big(c^2 \Big/ G_c\Big)[21G_c - E_c]\ddot{\tau}\Big\} \equiv 0
\end{aligned} \tag{16}
$$

By this means, the compatibility condition of Eq. (10) is obeyed in the formulation.

The appearance of the identity of Eq. (16) in the formulation under discussion is physically meaningful and is a result of the consistency between the nonlinear displacement fields in the soft core and its nonlinear acceleration fields. Therefore, in the present consistent formulation (unlike Ref. 2), all of the dynamic equilibrium equations contain the elastic and dynamic contributions, as anticipated on physical grounds. This structure of the dynamic equations also has advantages mathematically because one can effectively avoid the rank deficiency of the resulting mass matrix differential operator, as contained in Ref. 2.

The continuity conditions at any point $x = x_i$ along the span of a sandwich beam consist of seven kinematic and seven natural conditions through the cross section. The kinematic conditions express the compatibility between the left $(-)$ and right $(+)$ sides of the sandwich cross section at $x = x_i$ as follows:

$$u_{0t}^{(-)} = u_{0t}^{(+)} \tag{17}$$

$$u_{0b}^{(-)} = u_{0b}^{(+)} \tag{18}$$

$$w_t^{(-)} = w_t^{(+)} \tag{19}$$

$$w_b^{(-)} = w_b^{(+)} \tag{20}$$

$$w_{t,x}^{(-)} = w_{t,x}^{(+)} \tag{21}$$

$$w_{b,x}^{(-)} = w_{b,x}^{(+)} \tag{22}$$

$$\tau_{,x}^{(-)} = \tau_{,x}^{(+)} \tag{23}$$

The natural continuity conditions at $x = x_i$ are

$$u_{0t,x}^{(-)} - u_{0t,x}^{(+)} = N_{ti}/EA_t \tag{24}$$

$$u_{0b,x}^{(-)} - u_{0b,x}^{(+)} = N_{bi}/EA_b \tag{25}$$

$$w_{t,xx}^{(-)} - w_{t,xx}^{(+)} = M_{ti}/EI_t \tag{26}$$

$$w_{b,xx}^{(-)} - w_{b,xx}^{(+)} = M_{bi}/EI_b \tag{27}$$

$$
\begin{aligned}
&EI_t\Big(w_{t,xxx}^{(-)} - w_{t,xxx}^{(+)}\Big) - (1/2)bd_t\Big(\tau^{(-)} - \tau^{(+)}\Big) - \rho_t I_t\Big(\ddot{w}_{t,x}^{(-)} - \ddot{w}_{t,x}^{(+)}\Big) \\
&\quad + \rho_c A_c\Big\{(1/210)(11c + 39d_t)\Big(\ddot{u}_{0t}^{(-)} - \ddot{u}_{0t}^{(+)}\Big) \\
&\quad + (1/420)(13c + 27d_t)\Big(\ddot{u}_{0b}^{(-)} - \ddot{u}_{0b}^{(+)}\Big) \\
&\quad - (1/420)\Big(4c^2 + 22cd_t + 39d_t^2\Big)\Big(\ddot{w}_{t,x}^{(-)} - \ddot{w}_{t,x}^{(+)}\Big) \\
&\quad + (1/840)\Big[6c^2 + 13c(d_t + d_b) + 27d_t d_b\Big]\Big(\ddot{w}_{b,x}^{(-)} - \ddot{w}_{b,x}^{(+)}\Big) \\
&\quad + (1/840)(c/G_c)(2c + 9d_t)\Big(\ddot{\tau}^{(-)} - \ddot{\tau}^{(+)}\Big)\Big\} \\
&\quad = -m_t^{(-)} + m_t^{(+)} - P_{ti}
\end{aligned} \tag{28}
$$

$$
\begin{aligned}
&EI_b\Big(w_{b,xxx}^{(-)} - w_{b,xxx}^{(+)}\Big) - (1/2)bd_b\Big(\tau^{(-)} - \tau^{(+)}\Big) - \rho_b I_b\Big(\ddot{w}_{b,x}^{(-)} - \ddot{w}_{b,x}^{(+)}\Big) \\
&\quad - \rho_c A_c\Big\{(1/420)(13c + 27d_b)\Big(\ddot{u}_{0t}^{(-)} - \ddot{u}_{0t}^{(+)}\Big) \\
&\quad + (1/210)(11c + 39d_b)\Big(\ddot{u}_{0b}^{(-)} - \ddot{u}_{0b}^{(+)}\Big) \\
&\quad - (1/840)\Big[6c^2 + 13c(d_t + d_b) + 27d_t d_b\Big]\Big(\ddot{w}_{t,x}^{(-)} - \ddot{w}_{t,x}^{(+)}\Big) \\
&\quad + (1/420)\Big(4c^2 + 22cd_b + 39d_b^2\Big)\Big(\ddot{w}_{b,x}^{(-)} - \ddot{w}_{b,x}^{(+)}\Big) \\
&\quad - (1/840)(c/G_c)(2c + 9d_b)\Big(\ddot{\tau}^{(-)} - \ddot{\tau}^{(+)}\Big)\Big\} \\
&\quad = -m_b^{(-)} + m_b^{(+)} - P_{bi}
\end{aligned} \tag{29}
$$

$$\tau^{(-)} - \tau^{(+)} = 0 \tag{30}$$

Finally, seven boundary conditions for the upper and lower face sheets, as well as for the core at the left ($x = 0$) and the right ($x = L$) edges of the sandwich beam are, for the upper face sheet,

$$EA_t u_{0t,x} = \xi N_t \qquad \text{or } u_{0t} \text{ is prescribed} \tag{31}$$

$$EI_t w_{t,xx} = \xi M_t \qquad \text{or } w_{t,x} \text{ is prescribed} \tag{32}$$

$$
\begin{aligned}
&-EI_t w_{t,xxx} + (1/2)bd_t\tau + \rho_t I_t \ddot{w}_{t,x} - \rho_c A_c \\
&\quad \times \Big\{(1/210)(11c + 39d_t)\ddot{u}_{0t} + (1/420)(13c + 27d_t)\ddot{u}_{0b} \\
&\quad - (1/420)\Big(4c^2 + 22cd_t + 39d_t^2\Big)\ddot{w}_{t,x} \\
&\quad + (1/840)\Big[6c^2 + 13c(d_t + d_b) + 27d_t d_b\Big]\ddot{w}_{b,x} \\
&\quad + (1/840)(c/G_c)(2c + 9d_t)\ddot{\tau}\Big\} = \xi P_t + m_t \\
&\qquad\qquad \text{or } w_t \text{ is prescribed}
\end{aligned} \tag{33}
$$

For the lower face sheet,

$$EA_b u_{0b,x} = \xi N_b \qquad \text{or } u_{0b} \text{ is prescribed} \tag{34}$$

$$EI_b w_{b,xx} = \xi M_b \qquad \text{or } w_{b,x} \text{ is prescribed} \tag{35}$$

$$-EI_b w_{b,xxx} + (1/2)bd_b\tau + \rho_b I_b \ddot{w}_{b,x} + \rho_c A_c \times \Big\{(1/420)(13c + 27d_b)\ddot{u}_{0t} + (1/210)(11c + 39d_b)\ddot{u}_{0b} - (1/840)\Big[6c^2 + 13c(d_t + d_b) + 27d_t d_b\Big]\ddot{w}_{t,x} + (1/420)\Big(4c^2 + 22cd_b + 39d_b^2\Big)\ddot{w}_{b,x} - (1/840)(c/G_c)(2c + 9d_b)\ddot{\tau}\Big\} = \xi P_b + m_b \quad \text{or } w_b \text{ is prescribed} \tag{36}$$

For the core,

$$\tau = 0 \qquad \text{or } \tau_{,x} \text{ is prescribed} \tag{37}$$

where $\xi = -1$ for $x = 0$ and $\xi = 1$ for $x = L$.

Notice that, through the derived formulation, the actual two-dimensional problem in space is mathematically treated as one dimensional, which is of vital importance for the efficiency of numerical analysis.

In the next section, an efficient finite difference scheme for numerical solution of the derived consistent equations with arbitrary boundary conditions is introduced. Notice, however, that the semi-analytical approach, which uses harmonic assumptions through the span for main unknowns, can be conveniently used to find the free vibration response of a sandwich beam pinned at both upper and lower face sheets.

III. Numerical Approach

The consistent higher-order dynamic equations and associated boundary conditions derived in the preceding section can be represented in terms of differential operators as follows:

$$\begin{aligned} \boldsymbol{M}\ddot{\boldsymbol{v}} + \boldsymbol{K}\boldsymbol{v} &= \boldsymbol{f} \qquad \text{in} \qquad D \times D_t \\ \boldsymbol{m}\ddot{\boldsymbol{v}} + \boldsymbol{k}\boldsymbol{v} &= \boldsymbol{g} \qquad \text{on} \qquad \partial D \times D_t \\ \boldsymbol{v} = \boldsymbol{p}, \qquad \frac{\partial \boldsymbol{v}}{\partial t} &= \boldsymbol{q} \qquad \text{in} \qquad D \qquad \text{at} \qquad t = 0 \end{aligned} \tag{38}$$

In the present paper, finite differences are used to discretize the consistent formulation in Eq. (1). The derivation of a discretized formulation follows the methods decribed in Ref. 14. First, discretization in the space $(D_h \cup \partial D_h) \times D_{\Delta t}$ is accomplished, leading to a system of ordinary differential equations in time. For this purpose, a central difference scheme with fictitious grid points is employed.[15] The discretization in time is based on the implicit finite differences scheme[14] (⁝⁝), akin to the Crank–Nicholson method. The resulting formulation, which is discretized in space and time, reads

$$\begin{aligned} 2\boldsymbol{M}^h\boldsymbol{\varphi}^{hj+1} + (\Delta t)^2\boldsymbol{K}^h\boldsymbol{\varphi}^{hj+1} &= 2\boldsymbol{M}^h\boldsymbol{v}^{hj} + (\Delta t)^2\boldsymbol{r}_k^j \\ \boldsymbol{v}_k^0 = \boldsymbol{p}_k^0, \qquad \boldsymbol{v}_k^1 &= \boldsymbol{\varphi}_k^1 + (\Delta t)\boldsymbol{q}_k \\ \boldsymbol{v}_k^{j+1} &= 2\boldsymbol{\varphi}_k^{j+1} - \boldsymbol{v}_k^{j-1} \end{aligned} \tag{39}$$

The efficient time-marching scheme outlined earlier has been implemented in dynamic modules of the computer code FSAN, which are developed with the aid of the symbolic mathematical software Maple.[16] The computer code FSAN runs in the MATLAB® software environment.[17]

As already mentioned, the present formulation is one dimensional in space and, therefore, is numerically efficient. For comparison, the finite element solution of this problem will require the use of three- and two-dimensional elements for modeling the soft core and face sheets, respectively, and very fine vertical and planar meshes in the vicinity of the support zones and applied localized loads. Therefore, using a finite element model to produce results comparable in accuracy with the present formulation will require significantly more intensive and costly numerical calculations.

IV. Confirmation of the Consistent Analysis

The consistent higher-order dynamic theory is verified here, first, for free vibrations, and, second, for the forced response of a cantilever soft-core sandwich beam specimen, as shown in Fig. 2. The length and width of the specimen are $L = 260$ mm and $b = 59.9$ mm. The thickness of the face sheets is $d_t = d_b = 1.9$ mm, and the height of the core is $c = 34.8$ mm. The sandwich beam specimen is composed of steel face sheets and a polymer foam core (Table 1). The dimensions of the sandwich beam (wide beam) dictate the use of plane strain assumptions. Consequently, Young's moduli of the face sheets and the core in Table 1 are divided by $1 - \nu^2$, where ν is Poisson's ratio of the appropriate material, before they are used in the analysis.[9,18]

A. Free Vibration Response

A detailed analytical and experimental study of the free vibration response of the model sandwich beam in Fig. 2 was undertaken in Ref. 19. The measured natural frequencies and the finite element calculations from Ref. 19, and the numerical predictions based on the assumptions of Ref. 2, are compared with the results of the consistent analysis under consideration in Table 2.

Before the values in Table 2 are compared, note that the finite element (FEM) models used in Ref. 19 were based on eight-node plane strain quadrilateral elements, and these models did not accurately predict the first three thickness-stretch (symmetric) modes (modes 6–8 in Table 2). Moreover, because of the damping effects in the foam core, it was only feasible to measure the upper and lower

Table 1 Mechanical properties of the cantilever sandwich beam in Fig. 2

Component	Material	Young's modulus E, GPa	Shear modulus G, GPa	Poisson's ratio	Density ρ, kg/m^3
Face sheets	Steel	210	81	0.30	7900
Core	Divinycell H60	0.056	0.022	0.27	60

Table 2 Comparison of natural frequencies of the cantilever sandwich beam in Fig. 2

Mode	Frequency, Hz			
	Experiments[5]	FE[5]	Present theory	Ref. 2
1	——	165	165	165
2	544	512	512	511
3	950	913	912	910
4	1391	1379	1378	1373
5	1954	1939	1940	1928
6	——	2476	2392	2393
7	2350–2400	2509	2395	2398
8	——	2558	2425	2430
9	——	2567	2524	2534
10	2511	2608	2612	2590

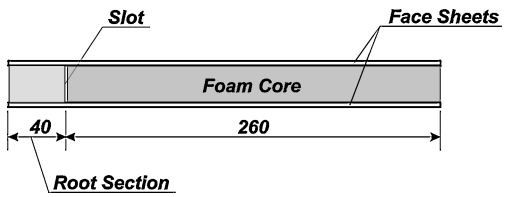

a) Elevation

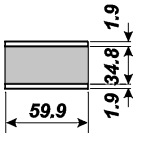

b) Cross section

Fig. 2 Schematic of the cantilever sandwich beam specimen (dimensions in millimeters).

bounds of the frequency range occupied by the symmetric modes 6–9 (Table 2).[19,20]

Comparison of the results in Table 2 shows that the natural frequencies of the shear vibration modes (antisymmetric modes 1–5 and 10) as predicted by the consistent analysis and the finite element calculations are quite similar. The small difference between these results and the predictions of the simplified higher-order formulation[2] grows with increasing mode number. Furthermore, the consistent analysis predictions match the measured symmetric frequency range more closely than both the finite element and the simplified higher-order formulation.

As already mentioned, the simplified higher-order approach of Ref. 2 can be used with confidence as far as the free vibration response is considered. Note, however, that the difference between the consistent and simplified higher-order predictions depends on the particular sandwich beam layout and might be several times greater than that in the present example.

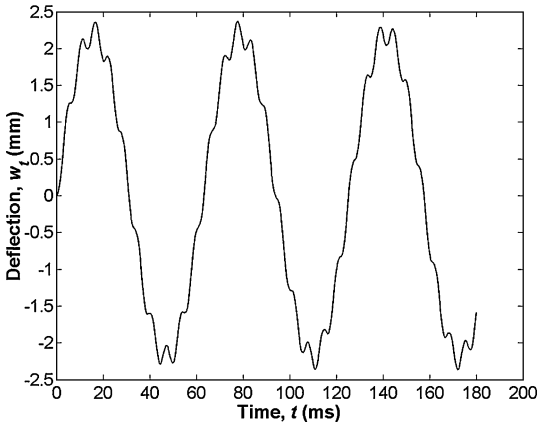

a) Large difference between the excitation and the first natural frequency, $\omega/\omega_1 \sim 0.1$

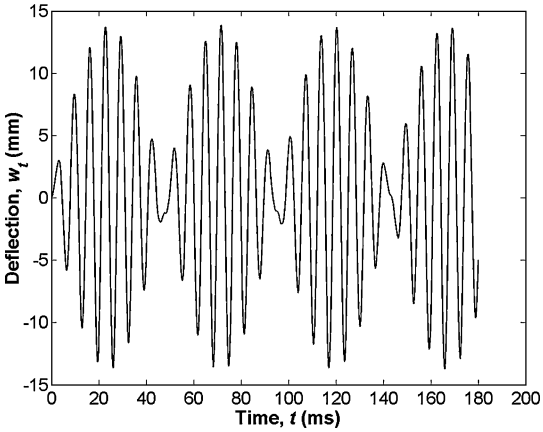

b) Beat phenomenon, $\omega/\omega_1 = 0.87$

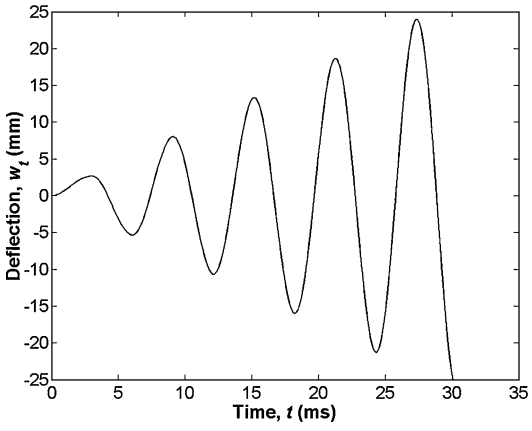

c) Resonance, $\omega \sim \omega_1$

Fig. 3 Time-domain response of the cantilever sandwich beam specimen in Fig. 2 subject to a localized harmonic load at the free end.

B. Forced Response

A sandwich beam subject to harmonic loading can be generally looked at as a simple undamped oscillator under the action of harmonic excitation. The response of such oscillators is well known[21] and can be used for the purpose of verification of the consistent analysis under discussion.

The forced time-domain response for the cantilever sandwich beam of Fig. 2 is considered in terms of the tip deflections of the

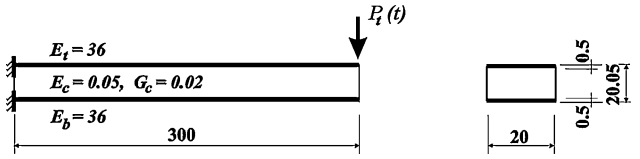

a) Layout

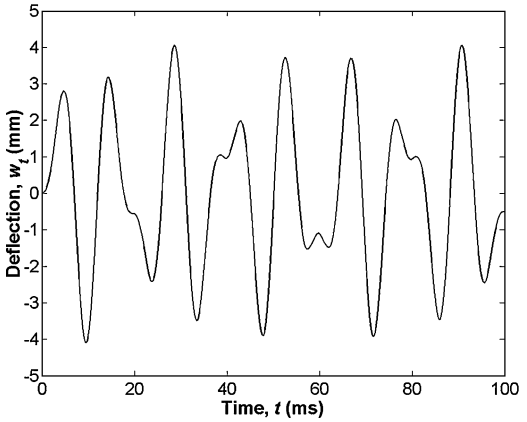

b) Time-domain response at the tip point of the upper face sheet for the excitation ratio of $\omega/\omega_1 \sim 0.6$

Fig. 4 Cantilever sandwich beam with isotropic face sheets (dimensions in millimeters and moduli in gigapascal).

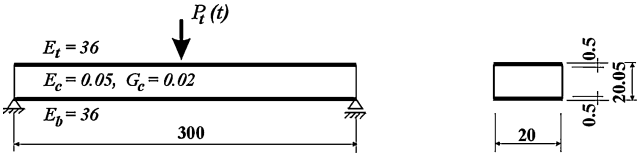

a) Layout

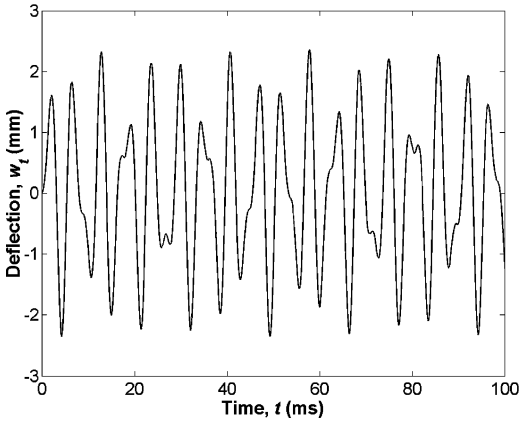

b) Time-domain response at the midspan point of the upper face sheet for the excitation ratio of $\omega/\omega_1 \sim 0.6$

Fig. 5 Sandwich beam with isotropic face sheets simply supported at lower face sheet only (dimensions in millimeters and moduli in gigapascal).

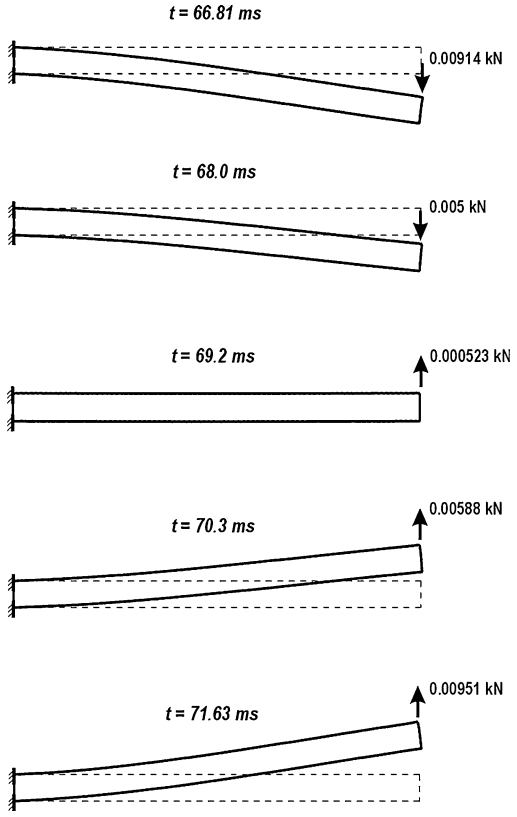

Fig. 6 Displacement patterns of the cantilever sandwich beam in Fig. 4a between the positive ($t = 66.81$ ms) and negative ($t = 71.63$ ms) peaks of the displacement amplitude at the tip point (Fig. 4b).

upper face sheet. The beam is subject to a harmonic localized (line) load $P(t) = 0.4 \sin \omega t$, which is applied to the free end of the specimen, and the response appears in Fig. 3. The three characteristic cases of the forced dynamic response, which correspond to different values of the excitation frequency, are considered. In the first case, shown in Fig. 3a, the excitation frequency ω is much lower than the fundamental frequency of the cantilever sandwich beam. When there is only a small difference between the excitation frequency and the fundamental frequency of the sandwich beam, a beat phenomenon arises, as shown in Fig. 3b. Finally, when the excitation frequency equal to the fundamental frequency of the specimen (Table 2), the resonant case results, as shown in Fig. 3c.

Note that the static deflection of the upper face sheet under the localized load $P = 0.4$ kN is $w_t \sim 2.19$ mm. For comparison purposes, this amplitude was kept unchanged for all of the cases in Fig. 3, despite the fact that the resulting tip deflections for the beat and resonance responses exceed the limit of the linear vibration assumptions, that is, the tip undergoes large displacements in the cases of beat and resonance responses. The results in Fig. 3 were obtained using a finite difference grid with a constant 0.5-mm interval between the grid points and a time interval of $\pi/30$ ms. Note particularly the accuracy of the consistent higher-order solution for the computationally challenging case of the beat phenomenon, where the wave $(\omega_n + \omega)/2$ is modulated by the wave $(\omega_n - \omega)/2$ (Ref. 21). The period of the modulating wave of a simple undamped oscillator for the frequency ratio used in the present example should be ~94 ms, which is closely matched in Fig. 3b.

V. Numerical Examples

In this section, examples of the forced response of soft-core sandwich beams subject to localized harmonic loads are presented to illustrate numerical applications of the developed formulation. Two important practical supporting cases are considered, including a cantilevered sandwich beam (Fig. 4a) and a sandwich beam simply

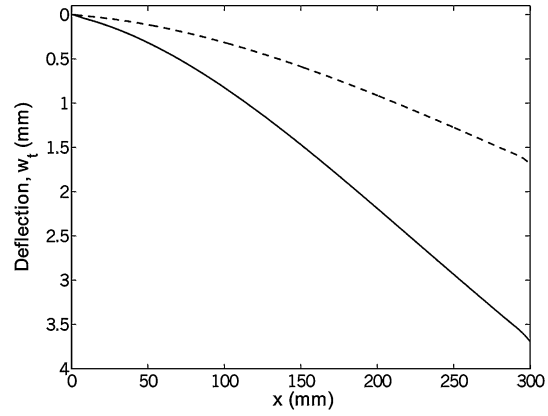

a) Vertical displacements of the upper face sheet

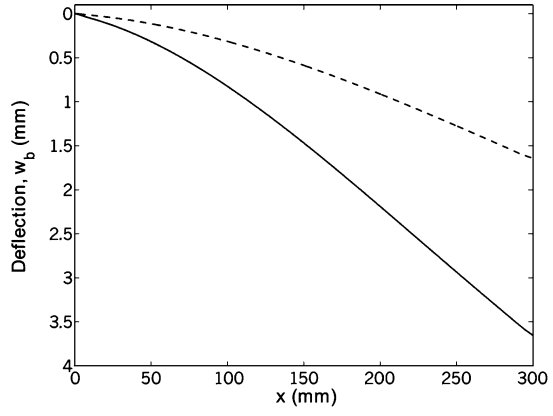

b) Vertical displacements of the lower face sheet

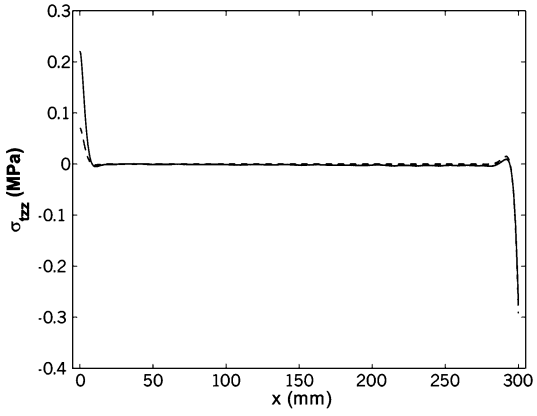

c) Normal stresses in the upper interface

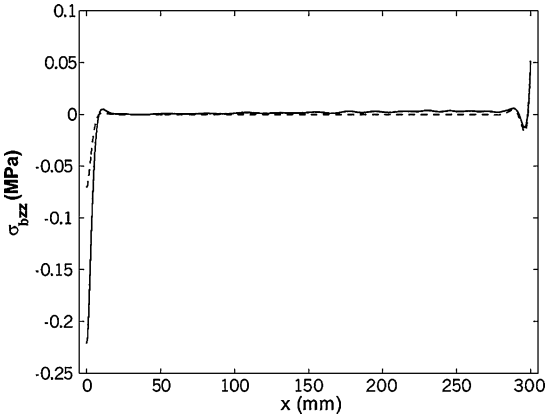

d) Normal stresses in the lower interface

Fig. 7 Comparison between the dynamic response of the cantilever sandwich beam in Fig. 4a at $t = 66.81$ ms (Fig. 6) and its static response at the tip point: ——, dynamic response and - - - -, static response.

supported at the lower face sheet only (Fig. 5a). The mechanical properties of the face sheets correspond to an isotropic material of density 4400 kg/m^3, whereas those of the core correspond to isotropic polymethacrylimide rigid foam of density 52.060 kg/m^3. (The free vibration analysis of these sandwich beams can be found in Ref. 4.)

To ensure a high degree of accuracy for the numerical analysis, the parameters of the finite difference scheme for both cases were

Table 3 Natural frequencies of the cantilever beam (Fig. 4a)

Mode	Frequency, Hz
1	129.9930
2	491.4857
3	997.4323
4	1468.7678
5	1939.0854
6	2153.1610
7	2392.1546
8	2842.2138
9	3280.0866
10	3714.4100

Table 4 Natural frequencies of the sandwich beam simply supported at lower face sheet only (Fig. 5a)

Mode	Frequency, Hz
1	289.9949
2	696.7346
3	1099.1359
4	1459.4748
5	1617.5716
6	1940.0701
7	2353.2043
8	2780.5021
9	3192.3868
10	3621.7602

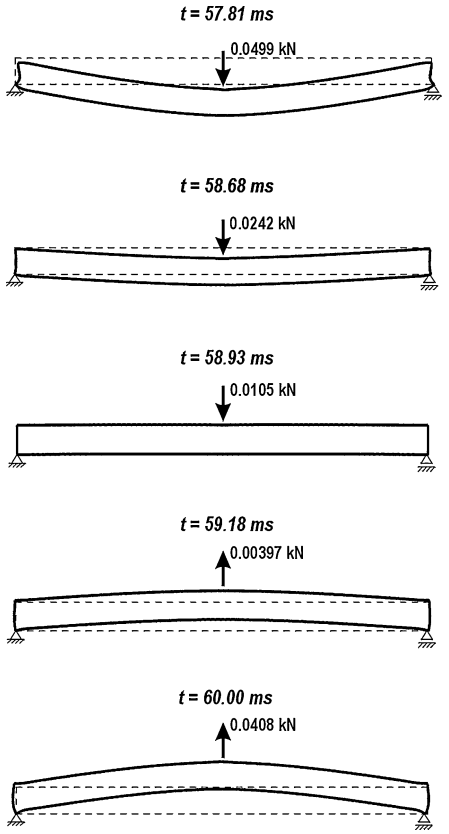

Fig. 8 Displacement patterns of the simply supported sandwich beam in Fig. 5a between the positive ($t = 57.81$ ms) and negative ($t = 60.00$ ms) peaks of the displacement amplitude at the midspan point (Fig. 5b).

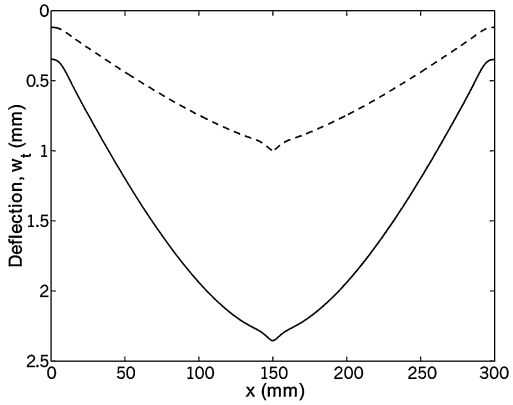

a) Vertical displacements of the upper face sheet

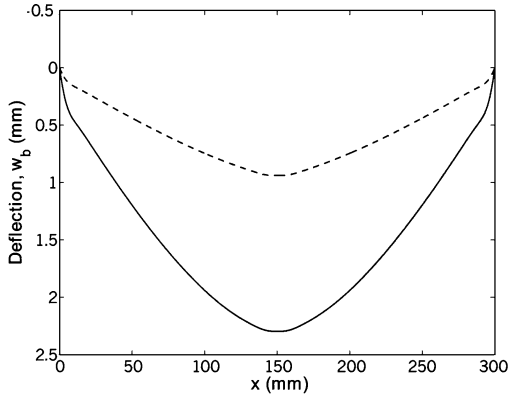

b) Vertical displacements of the lower face sheet

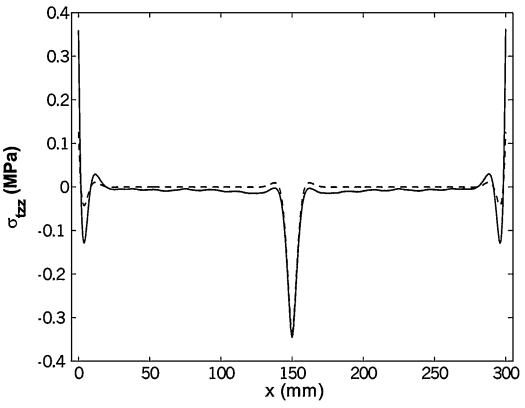

c) Normal stresses in the upper interface

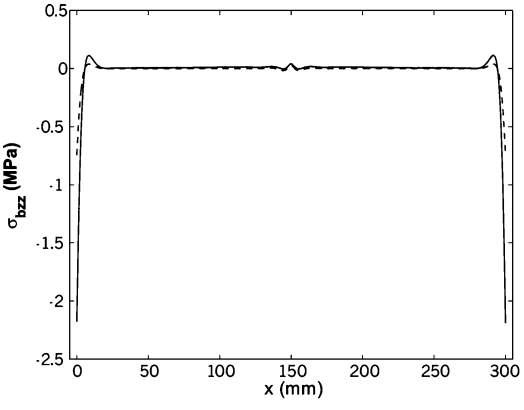

d) Normal stresses in the lower interface

Fig. 9 Comparison between the dynamic response of the simply supported sandwich beam in Fig. 5a at $t = 57.81$ ms (Fig. 8) and its static response at the midspan point: ——, dynamic response and - - - -, static response.

chosen to satisfy the tests in Fig. 3, including the values of the corresponding periods of motion. As a consequence, the numerical results were obtained using a finite difference grid with a constant 0.5-mm interval between the grid points and a time interval of $\pi/30$ and $\pi/60$ ms for the first and the second example, respectively.

The time-domain response of a soft-core cantilever sandwich beam subject to a localized sinusoidal load with amplitude 0.01 kN and frequency $\omega = 0.5$ rad/ms appears in Fig. 4b. (For reference, the first 10 natural frequencies of this beam are given in Table 3.) Note that the response in Fig. 4b is given in terms of the tip point displacement of the upper face sheet. The representative dynamic displacement patterns of the sandwich cantilever are given in Fig. 6. Figure 7 shows a comparison between the dynamic and static responses of the cantilever sandwich beam in terms of the vertical displacements of the face sheets and the normal stresses at the upper and lower interfaces. The dynamic response is given for one of the time instants where the local peak amplitude value is reached (Figs. 4b and 6). The ratio between the dynamic and static displacement amplitudes is high ($\sim$2.36) because the frequency of the exciting force in this example is $\sim$60% of the fundamental frequency of the cantilever sandwich beam under consideration (Figs. 7a and 7b). Figures 7c and 7d reveal that as a result of dynamic effects the normal (vertical) stresses in the face sheet–core interfaces, which are responsible for debonding failure of sandwich structures, increase dramatically at the clamped end of the beam, whereas they remain nearly at the level of response to quasi-static loading through the rest of the span, including the loaded unsupported edge.

A sandwich beam simply supported only at the lower face sheet appears in Fig. 5a. Note that this is the case of general boundary conditions, namely, the support conditions vary through the beam sections at the edges. The beam is excited at the midspan by the localized sinusoidal load with amplitude 0.05 kN and frequency $\omega = 1.1154$ rad/ms. This frequency corresponds to the same ratio between the excitation frequency and the fundamental frequency of a sandwich beam as in the earlier example (Table 4). The time-domain response of the sandwich beam in terms of the midspan vertical displacement of the upper face sheet appears in Fig. 5b, and the representative dynamic displacement patterns for this beam between the two local peaks in the time-domain response are given in Fig. 8. A comparison between the dynamic and static responses of the simply supported sandwich beam under consideration appears in Fig. 9. Unlike the earlier example, the difference between the vertical displacements of the upper and lower face sheets under the localized load is noticeable for both the dynamic and static responses, which can be seen from comparison of Figs. 9a and 9b. Furthermore, Figs. 9c and 9d show that, just as for the cantilever sandwich beam, the normal interface stresses significantly increase at the boundaries, whereas in the span, including the loaded middle point, the values remain nearly at the level of response to quasi-static loading.

VI. Conclusions

The consistent higher-order dynamic equations and the corresponding continuity and boundary conditions for sandwich beams with a transversely flexible core have been derived, taking into consideration the nonlinear acceleration fields in the core. In addition, a discretized formulation based on an efficient implicit finite difference scheme has been suggested and numerically validated.

A numerical study of the dynamic response of the cantilever and simply supported sandwich beams subject to the localized harmonic loads was undertaken. The study revealed that, as a result of dynamic excitation, the magnitudes of normal (vertical) interfacial stresses at the boundaries of a sandwich beam increase several times, whereas their values remain nearly at the level of response to quasi-static loading through the span, including the points of application of localized loads.

The present work provides an accurate and efficient tool for the analysis of sandwich beams with a transversely flexible core subject to dynamic loads of arbitrary type, including the practically important case of localized dynamic excitation. The use of the present formulation permits the structural analyst to capture the localized dynamic effects in a sandwich beam and to take into account closely modeled support conditions and the interaction between the two face sheets and core. This fidelity cannot be achieved using other sandwich models that use presumed vibration patterns, nonrealistic boundary conditions, and simplified assumptions for the dynamic behavior of a transversely flexible core.

Acknowledgment

The authors are grateful to the Merwyn C. Gill Foundation for support of this research.

References

[1]Chen, G., and Zhou, J., *Vibration and Damping in Distributed Systems*, Vol. 1, CRC Press, Boca Raton, FL, 1993.

[2]Frostig, Y., and Baruch, M., "Free Vibrations of Sandwich Beams with a Transversely Flexible Core: a High Order Approach," *Journal of Sound and Vibration*, Vol. 176, No. 2, 1994, pp. 195–208.

[3]Noor, F. K., Burton, W. S., and Bert, C. W., "Computational Models for Sandwich Panels and Shells," *Applied Mechanics Review*, Vol. 49, No. 3, 1996, pp. 155–199.

[4]Sokolinsky, V. S., Nutt, S. R., and Frostig, Y., "Boundary Condition Effects in Free Vibrations of Higher-Order Soft Sandwich Beams," *AIAA Journal*, Vol. 40, No. 6, 2002, pp. 1220–1227.

[5]Sokolinsky, V. S., Nutt, S. R., Frostig, Y., and Lesko, J.J., "Free Vibrations of Debonded Sandwich Beams—Higher-Order Theory Approach," *Sixth International Conference on Sandwich Structures*, edited by J. R. Vinson, Y. D. S. Rajapakse, and L. A. Carlsson, CRC Press, Boca Raton, FL, 2003, pp. 996–1005.

[6]Reissner, E., "Finite Deflections of Sandwich Plates," *Journal of Aeronautical Sciences*, Vol. 15, No. 7, 1948, pp. 435–440.

[7]Benson, A. S., and Mayers, J., "General Instability and Face Wrinkling of Sandwich Plates—Unified Theory and Approach," *AIAA Journal*, Vol. 5, No. 4, 1967, pp. 729–739.

[8]Frostig, Y., Baruch, M., Vilnay, O., and Sheinman, I., "High-Order Theory for Sandwich-Beam Behavior with Transversely Flexible Core," *Journal of Engineering Mechanics*, Vol. 118, No. 5, 1992, pp. 1026–1043.

[9]Allen, H. G., *Analysis and Design of Structural Sandwich Panels*, Pergamon, London, 1969, Chap. 2.

[10]Shames, H. I., and Dym, C. L., *Energy and Finite Element Methods in Structural Mechanics*, McGraw–Hill, New York, 1985, Chap. 7.

[11]Meirovitch, L., *Principles and Techniques of Vibrations*, Prentice–Hall, Upper Saddle River, NJ, 1997, Chaps. 4, 7, 8.

[12]Lanczos, C., *The Variational Principles of Mechanics*, Dover, New York, 1997, Chaps. 1, 2.

[13]Lopez, R. J., *Advanced Engineering Mathematics*, Addison–Wesley, Boston, 2001, Chap. 48.

[14]Marchuk, G. I., *Methods of Numerical Mathematics*, Nauka, Moscow, 1989, Chap. 1 (in Russian).

[15]Sokolinsky, V., "Nonlinear Behavior of Sandwich Structures with Transversely Flexible Core," Ph.D. Dissertation, Dept. of Civil Engineering, Technion—Israel Inst. of Technology, Haifa, Israel, March 2000.

[16]Heal, K. M., Hansen, M. L., and Rickard, K. M., *Maple 6 Learning Guide*, Waterloo Maple, Waterloo, ON, Canada, 2000.

[17]*MATLAB Reference Guide*, Ver. 6, MathWorks, Natick, MA, 2001.

[18]Reddy, J. N., *Mechanics of Laminated Composite Plates. Theory and Analysis*, CRC Press, Boca Raton, FL, 1997, Chap. 6.

[19]Sokolinsky, V. S., von Bremen, H. F., Lavoie, J. A., and Nutt, S. R., "Analytical and Experimental Study of Free Vibration Response of Soft-Core Sandwich Beams," *Journal of Sandwich Structures and Materials* (to be published).

[20]Jensen, A. E., and Irgens, F., "Thickness Vibrations of Sandwich Plates and Beams and Delamination Detection," *Journal of Intelligent Material Systems and Structures*, Vol. 10, No. 1, 1999, pp. 46–55.

[21]De Silva, C. W., *Vibration: Fundamentals and Practice*, CRC Press, Boca Raton, FL, 2000, Chap. 3.

A. Berman
Associate Editor